Investigation of influence of tool rake angle in single point diamond turning of silicon

Amir Mir[a], Xichun Luo[a], Kai Cheng[b], Andrew Cox[c]

[a]Centre for Precision Manufacturing, Department of Design, Manufacture and Engineering Management, University of Strathclyde, Glasgow, U.K

[b]Department of Mechanical, Aerospace and Civil Engineering, Brunel University, London, U.K

[c]Contour Fine Tooling Ltd., Stevenage, Herts, U.K

Xichun.luo@strath.ac.uk

Abstract

This paper presents an investigation of the effect of tool rake angle in single point diamond turning (SPDT) of silicon using experimental and simulation methods. Machining trials under the same cutting conditions were carried out using three different rake angle tools. In order to delve further into the rake angle effect on the output parameters including material removal, stresses, and crack formation, at the onset of chip formation and steady-state conditions, a simulation study using smoothed particle hydrodynamics (SPH) approach was performed. The simulations results were incorporated and found in good agreement with experimental observations. The results indicate that diamond tool wear rate and surface generation mechanism significantly vary using different rake angle tools. The continuance of compressive and shear deformation sequence at the chip incipient stage governs the high-pressure phase transformation (HPPT) as a function of rake angle and tool wear. The capability of diamond tool to maintain this sequence and required hydrostatic pressure under worn conditions is highly influenced by a change in rake angle. The proportional relationship of cutting forces magnitude and tool wear also differs owing to disparate wear pattern which influence distribution of stresses

and uniform hydrostatic pressure under the tool cutting edge. This subsequently influences structural phase transformation and therefore frictional resistance to cutting. Mainly frictional groove wear was found dominant for all diamond tools in machining of silicon.

Keywords: diamond turning, silicon, tool geometry, tool wear, chip formation

1. Introduction

Single crystal silicon is considered an ideal material in micro-photonics and weight-sensitive infrared applications due to its low mass density, high refractive index and low thermal expansion coefficient. High form precision and submicrometer surface finish are the key requirements of silicon-based functional surfaces for these applications. SPDT is an effective ultra-precision machining method to fabricate products with high form accuracy and optical surface finish without the need for subsequent polishing. SPDT of silicon is inherently a complex process that includes chipping, brittle fracture, ductile deformation, chemical reaction and phase transformation as a function of cutting parameters, materials orientation and tool geometry. The rapid wear of diamond tool is also a critical aspect that influences the surface integrity and operational cost of SPDT and need to be in limit and controlled.

A comprehensive understanding of coherence of silicon machining mode and tool geometry is imperative to achieve cost-effective and efficient SPDT by realising prolonged ductile mode machining at reduced tooling cost. The major reported work in the past reveal the significance of high-pressure phase transformation (HPPT) as a function of tool geometry which facilitates plastic deformation of silicon and accordingly influence tool wear mechanism [1-3]. The change in material properties of silicon as a function of HPPT significantly affects frictional resistance, chip

formation and chemical affinity consequently influencing tool wear during machining. Hence, there exist an interdependency of tool geometry and machining mechanism of silicon which affects machining performance.

The previous studies reveal that by careful selection of cutting parameters and tool geometry, ductile mode machining of silicon exploiting HPPT can be achieved [4-6]. From the tool geometry perspective, negative rake angle tools were found to generate high hydrostatic pressure required for structural transformation of silicon ensuing brittle to ductile transition (BDT). The increase of critical chip thickness was also claimed to increase with an increase in negative rake angle of the tool. Blake and Scattergood [5] performed SPDT of silicon and germanium using diamond tools with rake angles of 0°, -10° and -30°. They observed an increase of critical chip thickness from 0° to -10° rake and found a sharp increase in critical chip thickness at -30° rake. Yan et al. [7] observed an increase of critical chip thickness from 0° to -40° rake angle tools. Shibata et al. [8] conducted machining of silicon using -20° and -40° rake diamond tools at 100 nm and 1μm depth of cut. They found that rake angle effect diminishes at a depth of cut of 100 nm and becomes prominent from 100 nm to 1 μm in all crystallographic orientations. Zang et al. [9] suggested the importance of effective rake angle in association with cutting edge radius and depth of cut. Using 0° rake angle and -25° rake angle tools, they observed surface deterioration for an effective rake angle of~-60° rake using -25° tool and surface finish of 1 nm using lower negative effective rake angle. Diamond tools with negative rake angle are also assumed to provide cutting edge strength against any chipping or abrasive damage and consequently more control on an abrupt tool wear. Cutting edge sharpness of diamond tools considerably affect surface roughness and, therefore, considered also to be an important factor in achieving the optical surface quality of silicon.

Although negative rake angle is commonly agreed to be very important in achieving BDT of silicon, a clear disagreement pertaining to rake angles for ductile mode machining is found in the literature. In SPDT of silicon, diamond tools with intermediate negative rake angle from -20° to -50° are considered ideal for ductile mode machining. Positive rake angle tools are considered inefficient to produce required hydrostatic pressure for HPPT of silicon whereas negative rake angles greater than -50° are considered to cause obstruction in material removal. Although ductile mode machining of silicon has been realized using neutral 0° rake angle tools [10-12], intermediate rake angle, as well as extreme negative rake angles of -80° and-85° [5, 8, 13], maintaining ductile mode machining for longer cutting distance has not been considered in these studies. Also, a key factor to consider is the capability of worn tools of different rake angle tools to maintain HPPT for longer ductile mode machining. Therefore, there is a need to recognize an optimal rake angle that could maintain HPPT-based longer ductile mode machining and at the same time offer reduced tool wear.

In this paper, SPH-based numerical simulation study using Drucker-Prager (DP) material constitutive model was conducted in conjunction with machining experiments to investigate the effect of different rake angle tools. SPH method has been successfully employed in the machining of various ductile materials [14-16]. However, simulations of machining of brittle materials using SPH method are very few. Silicon, being one of the hardest and brittle materials never been simulated (in the author's knowledge) for cutting process using SPH. The simulation model of silicon using SPH method and constitutive DP model was proposed in this study to better predict the pressure-dependent plastic behaviour and crack formation of the material.

The first section of the paper describes the SPH formulation and its appropriateness for the machining model in comparison with Lagrangian mesh-based approach. A brief introduction of DP model was provided in the next section. The experimental plan and numerical simulation model of SPDT using SPH approach were presented in the following sections. The experimental and numerical simulation results were then evaluated by analysing the cutting forces magnitude and trend, chip formation, surface finish and tool wear.

2. Smoothed particle hydrodynamics formulation

SPH approach was first developed by Gingold and Monaghan in 1977 [17] for astrophysics applications. SPH uses kernel approximation to approximate field variables and properties in the domain as shown in Fig. 1. SPH approximate field variables at any particle by classical summation of smoothing function values of neighbouring particles within a sphere of influence. The length that defines the sphere of influence is based on smoothing length and it is the maximum distance to which the interaction can occur.

$$f(x) \cong \sum_{j}^{\infty} \frac{(m_b)}{\rho_b} f_b W(|X - X_b|, h) \quad ---- \quad (1)$$

Where $f(x)$ is a scalar function and subscript *b* represents the neighbouring particle of the particle *a* for which field variables need to be approximated. *W* is a smoothing Kernel function with radius h, called smoothing length. m_b and ρ_b are mass and densities of *b* particles. X_b is location of particle *b* with its value f_b.

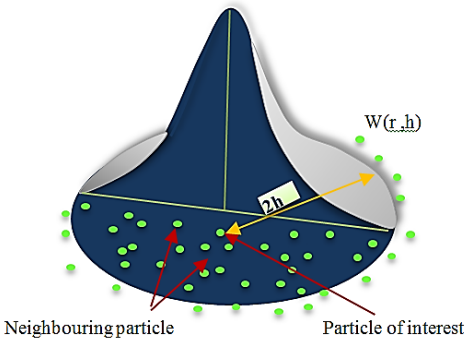

Fig. 1: SPH kernel approximation

Although Lagrangian mesh-based approach has been well researched in the FE simulations of machining of ductile materials [18, 19], simulation of hard and brittle materials such as silicon and silicon carbide using this approach is difficult and becomes impractical when using higher negative rake angle tools. This is not only because the pressure-dependent machining mechanism varies as a function of tool geometry and machining conditions; but also the true critical parameter values of physical and geometrical criteria for crack formation [20-22] along with pressure-dependent brittle damage models are difficult to be identified. Also, due to the negative rake angle of the tools, implementation of crack formation criteria along a dedicated layer becomes impractical. Due to the mesh-less nature and suitable particle connectivity, SPH offers continuous and discontinuous material removal due to plastic deformation and brittle fracture respectively without any separation criteria. The method presents a profound insight of variations in natural chip formation, hydrostatic pressure and stress distribution in brittle materials as a function of tool geometry and therefore, carries great significance. In comparison to the mesh-based Lagrangian formulation, SPH approach was found less efficient in studying processes with tensile instability or in small deformation processes [23].

Nevertheless, it has been found more expedient to study large deformation processes (as in cutting processes) than Lagrangian mesh-based approach. SPH approach has also been found to perform in an analogous manner to mesh-based approach following sensitivity analysis of particle resolution, mass-scaling and better in interface friction criteria [24].

In SPH method, all particles have a physical degree of freedom and each particle movement is influenced by its neighbouring particles located within the sphere of influence of radius r which is twice the smoothing length, 2h. The particles beyond the area of influence do not contribute to the intrinsic property of cohesion on the particle of interest. In SPH formulation, particles interact with each other based on defined constitutive equations and friction criteria is based on the internal friction between the particles instead of using theoretical friction parameters.

3. Drucker-Prager model

Drucker-Prager (DP) plasticity model has widely been implemented to simulate deformation behaviour of pressure-dependent materials including concrete and rocks. In pressure-dependent materials, a general trend is an increase in material strength with increasing confining pressure. Silicon behaves as a ductile material under specific higher hydrostatic stress zones. The strength of the silicon increases and the material deforms plastically under loading conditions.

In the von Mises yield criterion, the second deviatoric stress tensor J_2 is regarded solely a material yielding criteria without considering first stress invariant I_1. When considering pressure-dependent materials, the yielding sensitivity to hydrostatic stress tensor has not taken into consideration in this criterion. In 1952, Drucker and Prager [25] developed a yield criteria and incorporated the effect of hydrostatic

stress for pressure sensitive materials. This pressure-dependent model is known as Drucker-Prager model (also regarded as modified Mohr-Coulomb's model or extended von Mises model). Fig. 2 presents the DP yield surface which is the function of pressure and J_2 along with the Mohr-Coulomb model. The yield criterion of DP model is described as:

$$f(I_1, J_2) = \alpha I_1 + \sqrt{J_2} - d = 0 \quad \text{(2)}$$

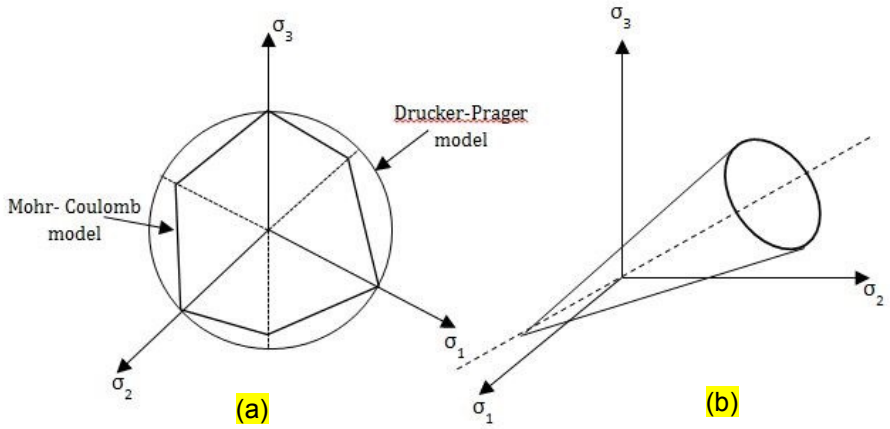

Fig. 2: Drucker-Prager model: (a) Mohr-coulomb and DP model in deviatoric plane (b) DP yield surface

In eq. (2) I_1 and J_2 are the first and second stress invariants, d is material cohesion and α is the hydrostatic-pressure sensitivity coefficient. The linear DP model can be represented by three invariants of stress tensor [26] and described as

$$f = t - p\tan\beta - d = 0 \quad \text{(3)}$$

where t and P are the deviatoric effective stress and equivalent pressure stress respectively and $\tan\beta$ represents the hydrostatic pressure-dependent yielding sensitivity of material. The parameter β is known as friction angle which represents the slope of the linear yield surface in meridional p-t stress plane.

4. Experimental Plan

The SPDT of silicon with high surface quality and minimal sub-surface damage is only possible with stiff machine tools. In this research, machining trials were carried out on an ultra-precision diamond turning machine – Nanotech 250 UPL (Moore Nanotech system) which is equipped with air-bearing spindle offering low friction and less heat generation and hydraulic motional slides of high stiffness.

Single crystal diamond tools in dodecahedral crystal orientation were used to machine P-type silicon wafers of (111) crystal orientation. Fig. 3 shows the machining setup and SEM image of negative rake round edge tool used in SPDT of silicon. Three different negative rake angle tools were used in order to investigate the effect of rake angle on surface generation mechanism of silicon.

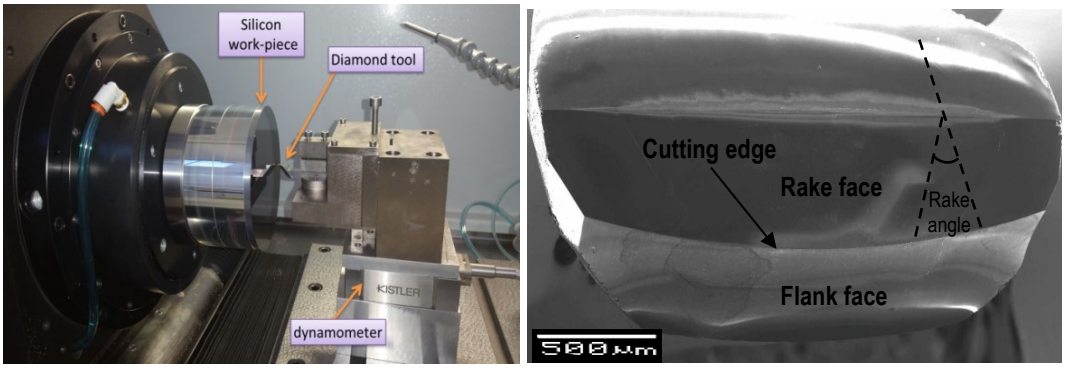

Fig. 3: Machining setup of SPDT of silicon and SEM image of the new tool

Cutting edges as well as rake and flank faces of new diamond tools were carefully examined under SEM for any prior damage. The selection of cutting parameters and coolant was based on previous established research work of diamond turning of silicon to attain high optical quality machining [27]. Large nose radius tools were used as they provide strong edge geometry to withstand higher frictional resistance and higher cutting forces. Critical depth of cut as well as critical feed rate for brittle to ductile transition were also found to increase with increasing nose radius during

SPDT of brittle materials [28, 29].Table 1 presents tools and workpiece details and machining conditions adopted in the experimental work.

Table 1: Experimental machining data and conditions

Silicon wafer	Diamond tools	Cutting parameters
Optical grade silicon, polished Round Orientation =<111> +/-5° Diameter = 100 mm Thickness = 5 mm Sample purity = 99.999%	Orientation = Dodecahedral Nose radius = 5 mm Rake/Clearance angle: • Tool1= -25°/10° • Tool2= -30°/10° • Tool3 = -40°/25°	Spindle speed =1200 rpm feed rate = 1 µm/rev Cutting speed = 3-6.2 m/sec Depth of cut = 10 µm Coolant = Distilled water

Each silicon wafer was divided into two zones: facing and plunge zones. The facing cuts were performed repeatedly with the same 10 µm depth of cut and 1 µm/rev cross-feed until the onset of the brittle fracture. In the reiteration of facing cut, the tool retraction radius for each following facing cut was reduced by 1 mm.

Cutting forces were monitored and recorded using a three-component Kistler dynamometer 9256. An advanced data acquisition system with Dynoware software was used to get the Fx, Fy and Fz forces. Surface roughness was measured using a white light interferometry (Zygo Newview 5000) for each iteration of facing cuts. The tools were monitored after machining under SEM for any induced wear or damage caused by the machining trials. The cutting distance was calculated for each diamond tool before the onset of brittle fracture to measure tool performance.

Confirmation trials were also performed using the same tool and workpiece geometries, orientations and machining conditions. The methodology for monitoring tool conditions, cutting forces and surface finish were the same adopted in the first trial.

5. SPH Cutting Simulation Model

In machining operations, concurrently occurring phenomena including material removal, HPPT, stresses as well as crack nucleation and propagation, at the onset of chip formation occur in an infinitesimal fraction of time and scale. It is nontrivial to understand these output variables state and conditions as it significantly influences tool geometry performance as well as tool wear. However, it is difficult to measure and observe these output variables in experimental conditions. In this research, SPH-based simulations of orthogonal cutting of silicon were carried out using finite element (FE) software Abaqus to study these output variables.

In order to corroborate the rake angle effect observed during the experimental study, SPH simulations of SPDT of silicon were performed under the same cutting conditions using different rake angle tools. The tool was modelled with eight-noded C3D8R elements using Lagrangian element-based mesh and was kept rigid due to significantly high modulus of diamond compared to silicon. The workpiece was modelled as a deformable part with PC3D particles to handle large deformation during the cutting process. The workpiece dimensions were kept at (200x100x50) μm. The bottom of the workpiece was retained in all directions. In cutting simulation, the tool moves with similar experimental cutting velocity in the negative x-direction. Fig. 4 shows a cutting simulation model used in this study.

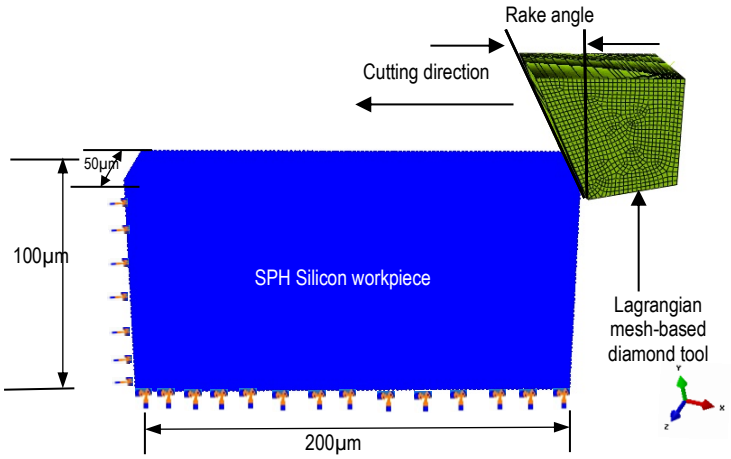

Fig.4: SPH cutting simulation model of silicon

In order to examine the rake angle effect, cutting simulations were performed with four different rake angle tools using the same cutting conditions adopted in experiments. Although diamond tool with +5° rake angle was not used during the experimental trials, it was included in the simulation study to provide the comparison of chip formation and distribution of different stresses using positive and negative rake angle tools. Table 2 shows the cutting parameters used in the simulation study.

Table 2: Cutting parameters used in SPH simulation

	Rake/clearance angle	Workpiece size (µm)	Cutting speed (m/s)	Depth of cut (µm)
1	+5°/10°	200x100x50	6.3	10
2	-25°/10°			
3	-30°/10°			
4	-40°/10°			

The Drucker-Prager (DP) constitutive material model was adopted in this study to simulate the machining behaviour of silicon. The compressive yield strength of silicon is higher compared to its tensile strength [30] which is an elementary criterion of using DP model. Table 3 lists the material properties and DP model parameters of silicon [31] used in SPH cutting simulation.

Table 3: Material properties of silicon	
Density, ρ	2330 kg/m^3
Elastic modulus, E	146 GPa
Poison's ratio	0.27
Friction angle (β)	26°
Dilation angle (Ψ)	20°
Flow stress ratio, k	0.82

6. Results and discussions

SPDT of silicon using three different rake angle tools was carried out until the onset of brittle fracture. Fig. 5 shows the diamond turned silicon wafer with severe brittle fracture appeared in a threefold symmetry pattern. Due to the high anisotropy of single crystal silicon, machining mode is dependent on crystallographic orientation based on the orientation of dislocation and slip system relative to cutting direction. Therefore, in face turning of silicon with (111) orientation, threefold pattern of cloudy surface has been reported frequently [28, 32].

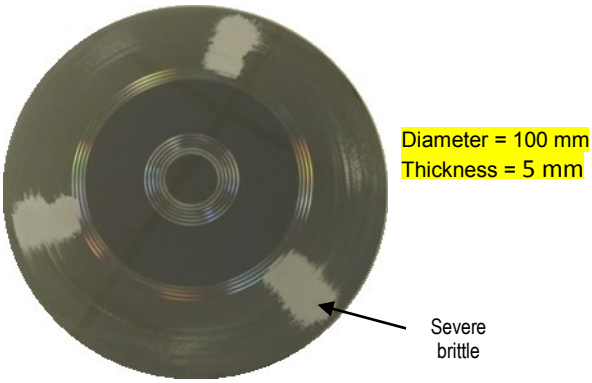

Fig.5: Brittle fracture in 3-fold pattern on silicon

The results of output parameters obtained using different rake angle tools were recorded and discussed in the following sections. Tool rake angle is considered as a determining factor of surface generation mechanism in SPDT of silicon. In order to investigate the rake angle effect, cutting forces, stresses, hydrostatic pressure, chip formation and tool wear were measured and analysed for different rake angles.

6.1. Cutting forces

Cutting forces are considered as the most accredited indicator to characterise material removal modes, frictional resistance to cutting, as well as tool wear. Cutting forces were recorded in each facing cut for all rake angle tools. Although cutting temperature has a significant effect on cutting forces magnitude as high cutting temperature during machining results in softening of the material as well as change of machining mode, cutting temperatures during SPDT of silicon were not recorded high enough [33, 34] to cause any softening of material, and therefore shouldn't affect the cutting force magnitude significantly.

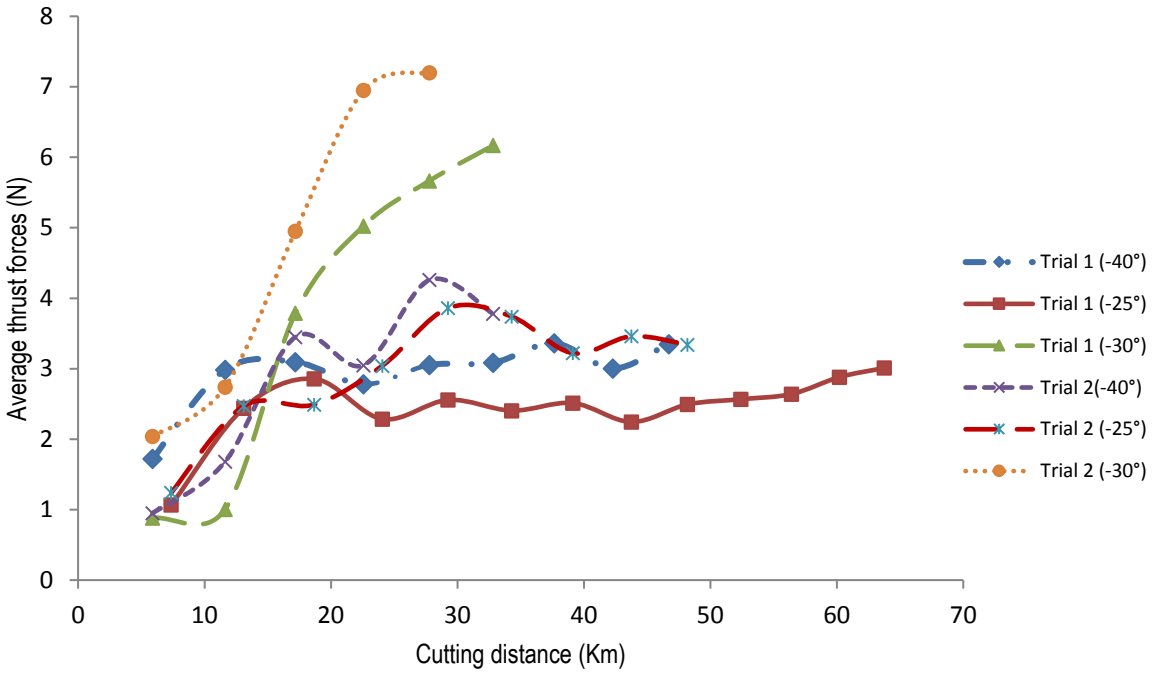

Fig. 6: Thrust forces trend with cutting distance

Fig.6 presents average thrust forces recorded in trial 1 and trial 2 with respect to cutting distance for different rake angle tools. In both the trials, diamond tools with -25° rake angle attained the longest cutting distance before the onset of brittle fracture followed by -40° rake tools. With the increasing cutting distance, tool wear

develops which results in an increase of cutting forces. Cutting forces trend suggest the maximum tool wear rate from 0-20 km and then gradual frictional wear for the rest of the cutting distance. This phenomenon substantiates the understanding of higher wear rate of sharp edges of new tools due to stress concentration in the cutting-edge zone. For -30° rake angle, the tool achieved the least cutting distance with the sharp rise of cutting forces. Similar cutting forces behaviour of -30° rake tool was recorded during the confirmation trials.

Fig. 7 presents the tangential to thrust force ratio for the three different rake angle tools. Although for the -30° rake tool, the thrust forces were found higher than tangential forces, the relative magnitude of the tangential force is higher than the other two tools. This explains the dominant cutting phenomenon with reduced compressive stresses and hence early brittle fracture.

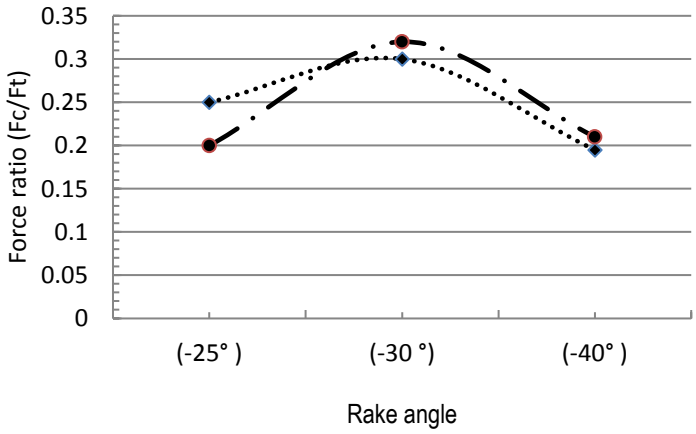

Fig. 7: Force ratio trend with decreasing rake angle

Machining forces were measured in SPH cutting simulation of silicon using different rake angle tools. Fig. 8 presents a comparison of experimental and simulation-based mean thrust forces. A good correlation of forces can be seen for -25° and -40° rake angle tool except -30° rake tool for which the percentage difference increased to 30% between experimental and simulation values. This high difference could possibly be

due to the resulting cutting force vector coincide or close enough to the preferred direction of silicon crystal structure in (111) direction and require further investigation.

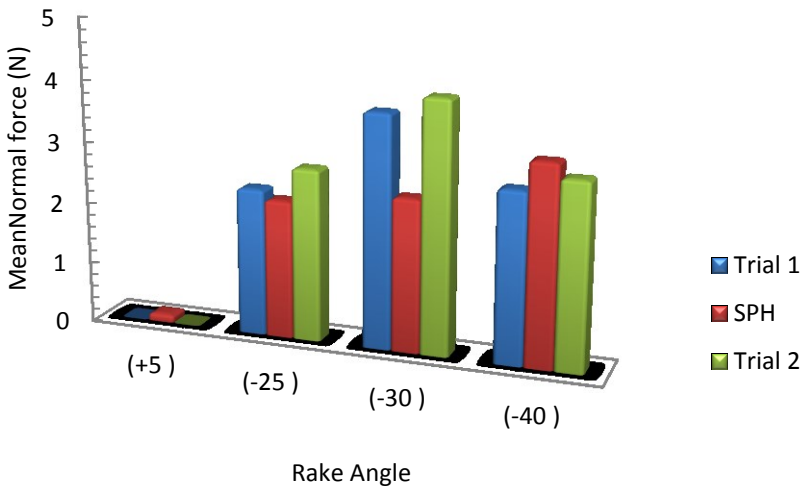

Fig. 8: Comparison of Experimental and simulation cutting forces

6.2. Stress distribution and chip formation

The mechanics of chip formation during machining can be better understood by understanding the deformation conditions in the chip formation zones. Any change in tool geometry significantly influences shear stresses, strain and temperature distribution during chip formation. Fig. 9 presents the schematic of cutting process in SPDT process.

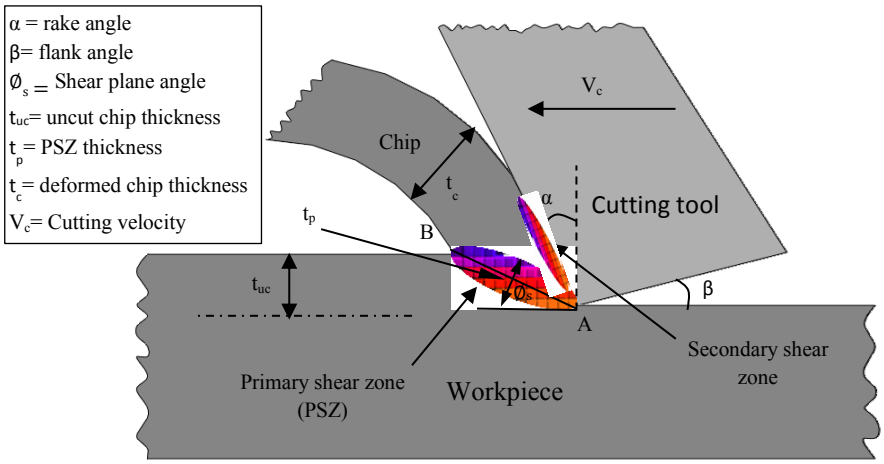

Fig. 9: Schematic of chip formation in SPDT

The geometry of the primary shear zone (PSZ) is governed by the shear plane angle ($Ø_s$) and the ratio of the length of PSZ (L_{AB}) to its thickness (t_p). Fig. 10 presents the change of shear plane length and shear angle with the change of rake angle. With the increase of shear zone area, the strength of the material increases and hence increases in deformation energy. It can be noted that shear angle reduces with the increase in negative rake angle from -25° to -40°. Although shear plane area and shear strain magnitude increase with increasing negative rake angle tool, the length of PSZ decrease from -25° to -30° and then increases for -40° tool.

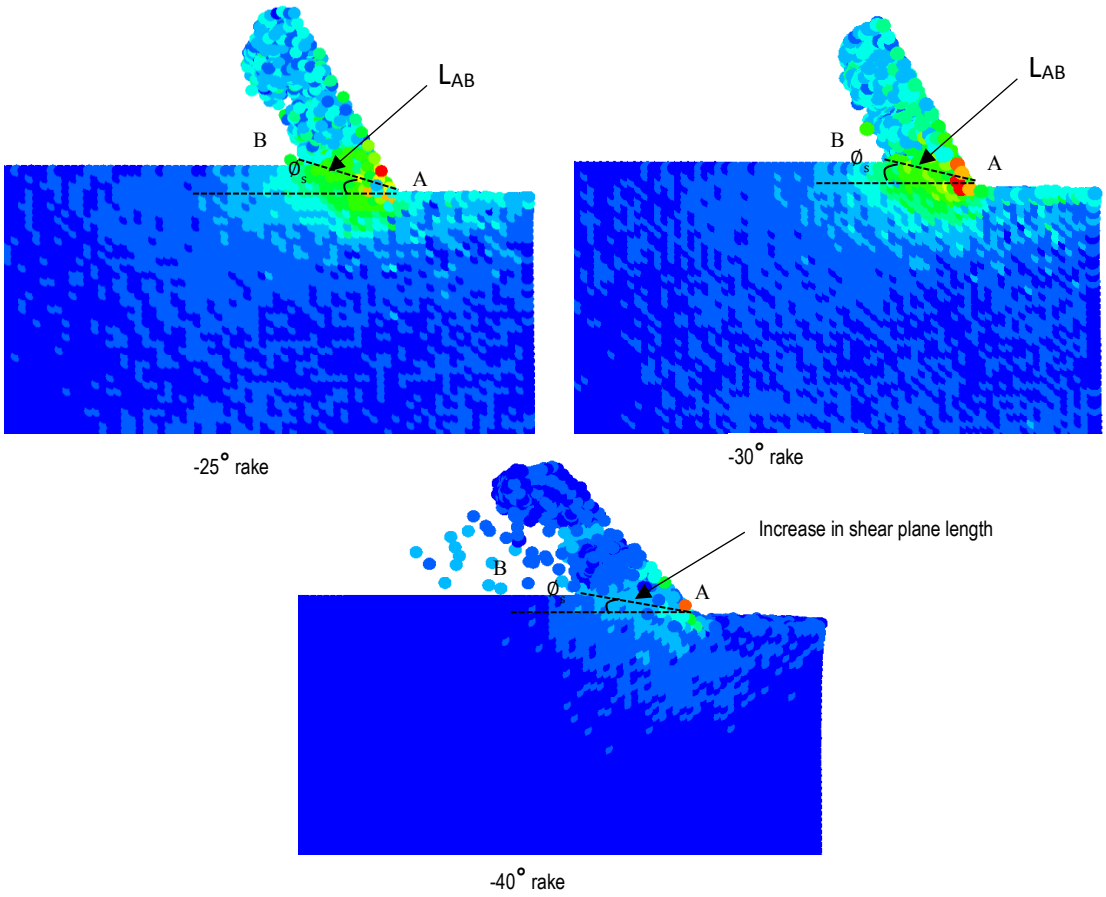

Fig. 10: Change of shear plane length and shear angle

Stresses and pressure distribution and chip formations were also investigated in cutting simulation with different rake angle tools. Von Mises stresses were found to increase beyond the theoretical yield strength of silicon for all negative rake angle tools and continuous material removal observed throughout the cut. For the +5° rake angle tool, although, at first contact, the maximum von Mises stress reached 10 GPa at tool-chip interface in the primary deformation zone, material separation initiated by a crack in front of tool tip propagating in the forward direction. Fig. 11 shows the crack formation and surface damage on the removal of chip segment using positive rake tool.

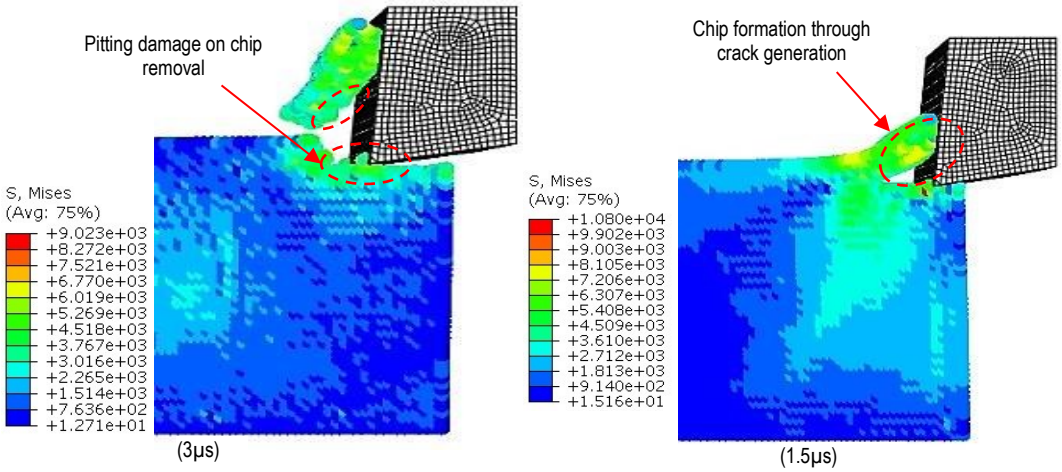

Fig. 11: chip formation using +5° rake angle

Bending stresses develop at the bottom surface of the chip and broken chips can be observed from the initiation to the concluding stage of chip separation. An average hydrostatic static pressure of 4 GPa was recorded for +5° tool compared to negative rake angle tools. The average hydrostatic pressure of 15 GPa, 14 GPa and 19 GPa was recorded for -25°, -30°, and -40° tool respectively. Due to lack of required hydrostatic pressure under the tool tip for +5° tool, chip separation occurs due to developed cracks and result in discontinuous material removal. On the removal of chip segment, surface ahead of the tool undergoes pitting damage under the cutting depth. The direction of developed crack also defines the final machined surface as any crack propagation angle towards the final machined surface result into brittle damage.

Fig. 12 shows the von Mises stresses and the variation of chip formation for different negative rake angle tools. An imperative aspect to notice was the variation of stresses with an increase in negative rake angle. In general, an increase in stresses is likely to be predicted with an increase of negative rake angle. Nevertheless, at contact stage, von Mises stresses were found higher for -25° rake than -30° and -40° rake tools. Since lower negative rake tools are likely to initiate chip formation along with compressive stress at first contact with the workpiece surface, shear stresses

remain dominant than compressive stresses. With the increasing negative rake, compressive stresses surpass shear stresses at initial contact with the workpiece surface.

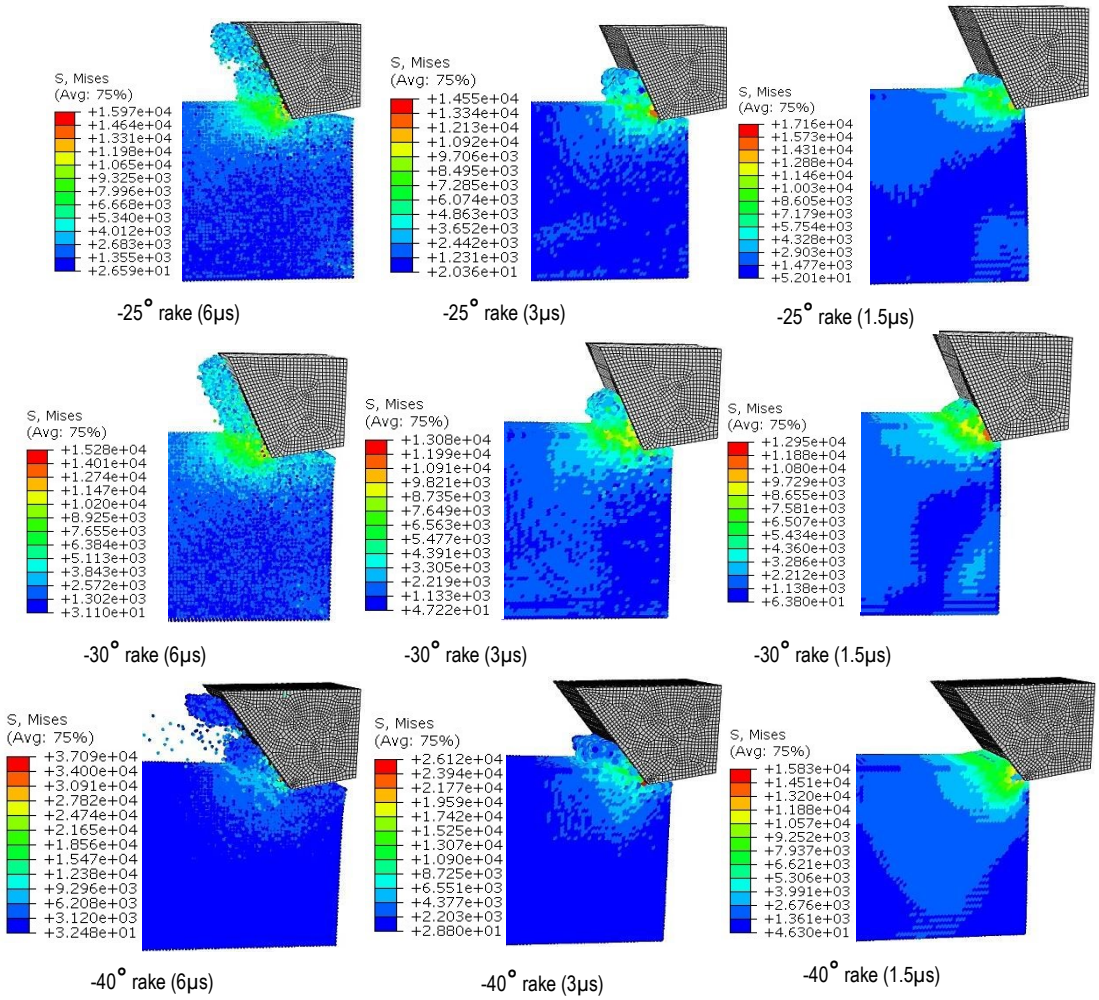

Fig.12: Von-Mises stresses (MPa) and chip formation for different rake angle tool from initial to steady-state

At steady-state conditions, developed stresses for -40° rake tool significantly increased than other two tools. This phenomenon attributed to the increase of yield strength of silicon with increasing hydrostatic stress using higher negative rake angle tools. However, for -30° rake angle, von Mises stresses at initial and steady-state conditions were found lower than the -25° rake tool. This behaviour validates the shortening of shear plane length using -30° tool in Fig. 10 which results in a

decrease of von Mises stresses. The failure stresses can also influence by the intensity and sequence of compressive and shear stress from incipient to steady-state condition as a function of rake angle. Also, the type of chip formation ahead of the tool contributes to the normal and shear stress distribution on the tool rake face and cutting edge.

In SPDT of silicon, chip contour in secondary deformation zone (SDZ) also influence by the unloading conditions. In machining, the unloading mainly transpires at machined surface behind the tool edge as well reduce loading condition develop at tool-chip interface in SDZ. This change affects machined surface and chip contour in SDZ which can be observed in Fig. 12. For the -25° tool, the chip breaks into segments and particles in SDZ. The severity of the disintegration into particle was observed higher for -40° compared to -25° tool indicating high unloading effect. For -30° tool, the chip remained continuous without breakage. In order to further investigate this behaviour, pressure distribution study was performed.

6.3. Chip geometry

A good correlation of chip formation was found in experimental and SPH machining studies of silicon. Fig.13 shows the SEM images of silicon chips collected in the first facing cuts for the three rake angle tools. Chips were formed in the combination of continuous, broken and powder form with different thickness. For -25° rake angle tool, chips were mainly formed in combination of continuous and broken chips along with dominant powder form. Smoother and longer ribbon type chips were observed using -30° rake angle tool. Similar behaviour can be observed in SPH simulations where for -30° tool, chips remain continuous in the SDZ. Whereas for -25° and -40°, chips were found to break into particles due to unloading effect.

For both -25° and -40° tools, although the chips were found in the combination of ribbon, broken and powder form, the chip shapes were observed distorted using -40° tool. The distortion could possibly due to the flow of chip under the tool with high compressive stresses.

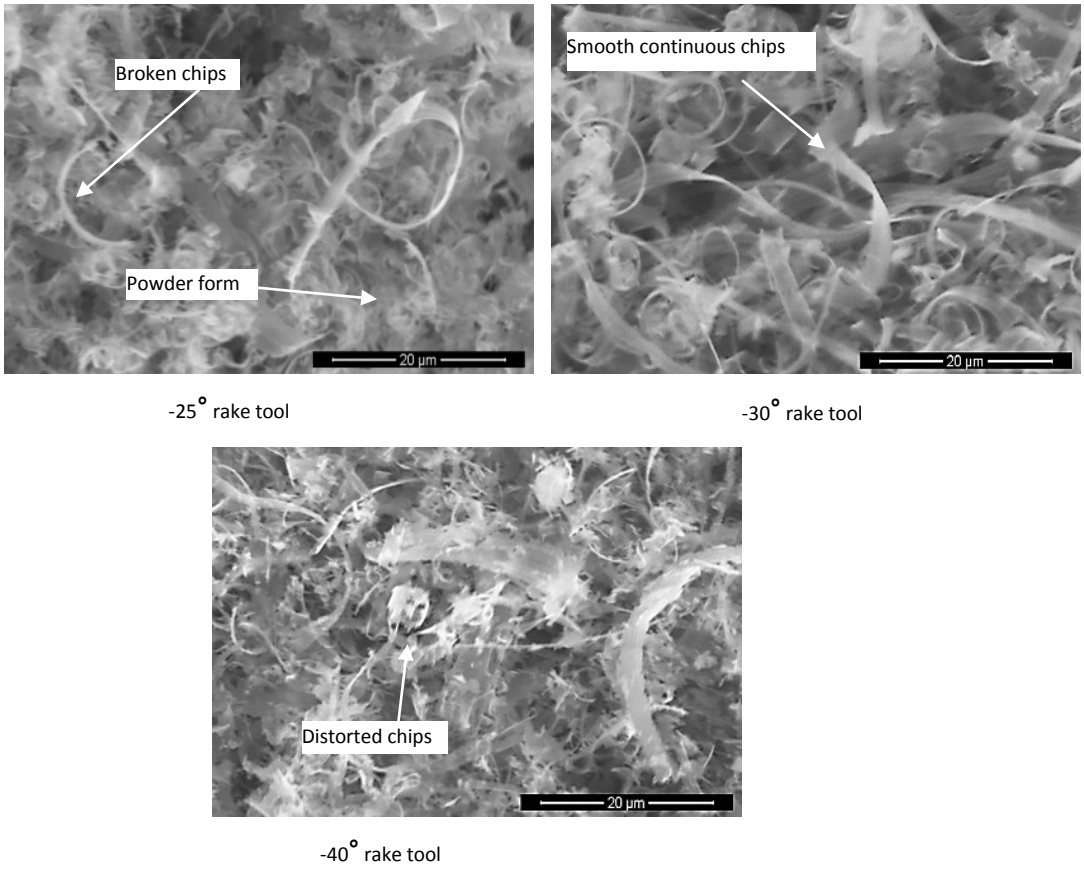

Fig.13: SEM images of silicon chips for different rake angle tools

Tool wear in SPDT of silicon has previously been attributed to the formation of SiC and diamond-like carbon particles [12], or dynamic hard particles [35] scratching or ploughing on the tool flank face forming groove wear. The chemical reaction of diamond carbon and silicon at a high cutting temperature of 959K [34] in the presence of oxygen may lead to the formation of silicon carbide. The formation of SiC due to the silicon-carbon reaction is a significant factor to investigate as it affects material removal mechanism and tool wear. Energy-dispersive X-ray spectroscopy

(EDX) analysis was performed on all the chips collected during all facing cuts using three different rake angle tools. Chips collected during both ductile machining and brittle machining were analysed for the presence of SiC. No trace of SiC formation detected in all the chips analysed during EDX analysis. Fig. 14 presents the EDX spectrum of collected silicon chips in SPDT study. The presence of carbon in the EDX analysis was determined as carbon contamination in the chamber.

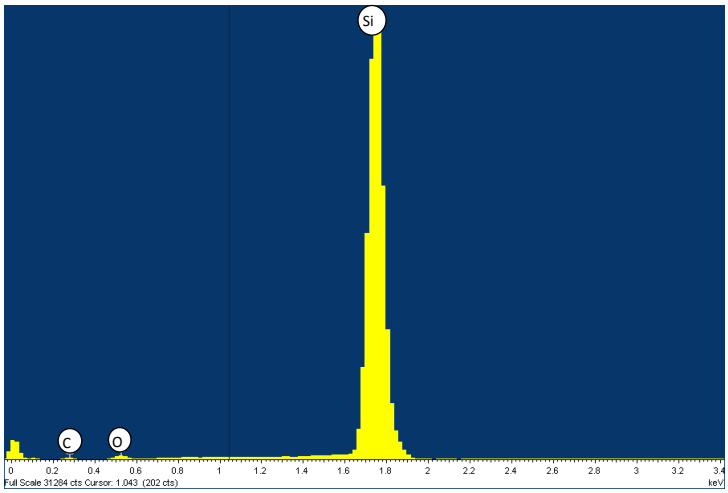

Fig. 14: EDX spectrum of silicon chips obtained in SPDT study

6.4. Tool wear

Tool wear study carried out using scanning electron microscopy (SEM) and diamond tools were inspected for any initial damage prior to machining. The results were evaluated by comparing before and after SEM measurements. Previous studies suggest that abrasive, chemical and thermal wear mechanisms are the possible wear in SPDT of silicon [11, 12, 36]. Typically multiple tool wear mechanisms can be active but only one tool wear mechanism is dominant for a specific workpiece material and for a certain cutting regime. In both the trials of this study, mainly frictional groove wear at flank face was found dominant for all the tools. Tool wear started at the cutting edge shifting the edge towards the rake face and making

grooves on the flank side of the tools. This is due to maximum stress intensity and maximum friction found at cutting edge and trailing flank surface. For the -25° diamond tool, the pitting damage was also observed at the rake face of the tool in both the trials. The pitting damage was found mainly due to chipping phenomenon. For the other two tools, no crater wear was observed in both the trials. Fig. 15 shows the SEM images of diamond tool indicating crater wear and flank wear of -25° diamond tool.

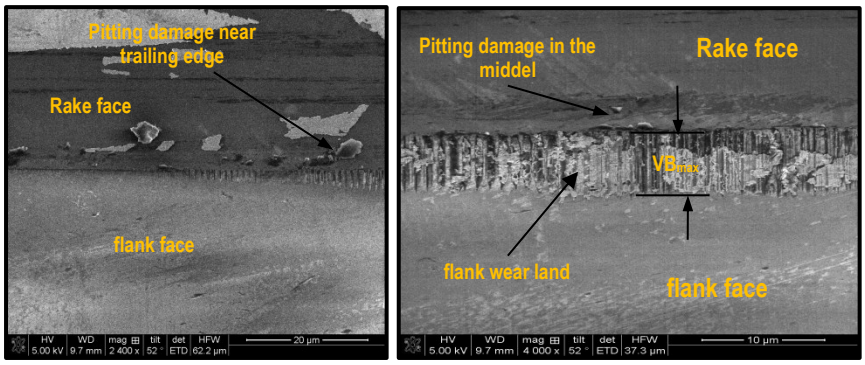

Fig. 15: SEM image of flank and crater wear of -25° tool

Fig. 16 presents the frictional groove wear contour in all three tools appeared after machining silicon. Uniform width of flank wear land was found in the middle of cutting edge narrowing down in the form of the curve towards the edges. The flank wear land width for -40° rake tool was recorded 3 µm much smaller than 6.5 µm and 7.5 µm for -30° and -25° rake angle tools respectively. This possibly due to the clearance angle of 25° compared to 10° for the other two tools.

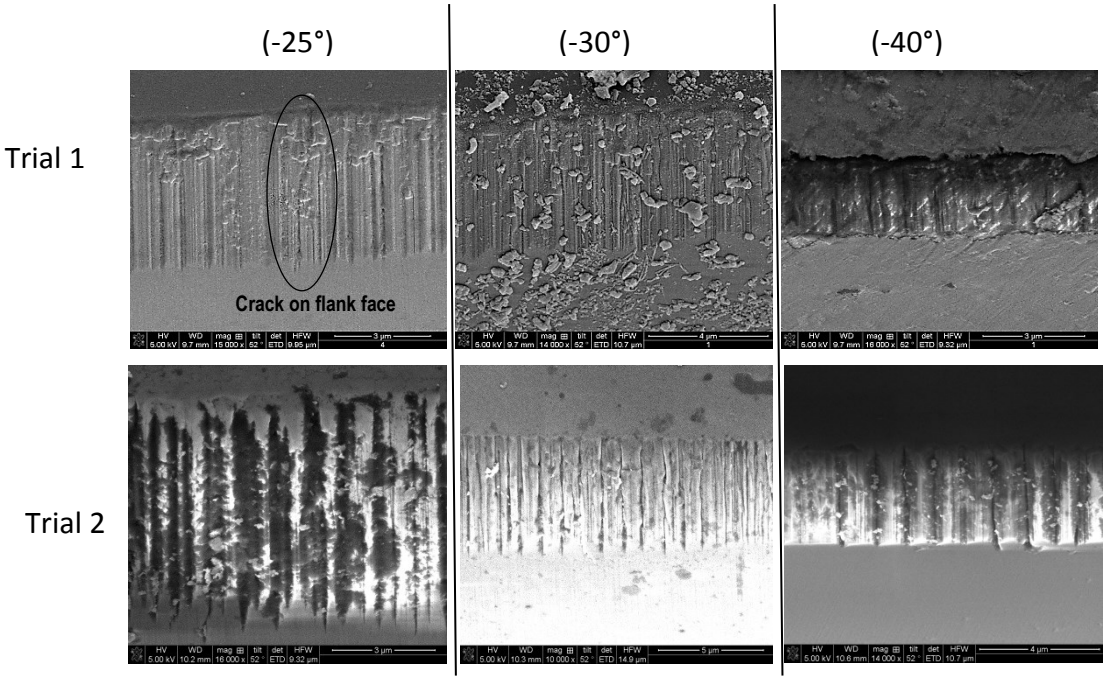

Fig.16: Tool wear pattern for different rake angle tools in trial 1 and trial 2

A crack found to appear in the wear land area of -25° rake angle tool connecting rake and flank faces of the tool. Although high thermal conductivity of diamond tool and silicon along with coolant significantly contributes to reducing the cutting temperature, with the increased frictional resistance due to wear, cutting temperature may increase significantly. Diamond tools tend to undergo thermal cracking and chemical wear at higher cutting temperatures. The crack appeared in the wear land of -25° rake tool can possibly be the result of thermal cracking, rapid heating and cooling, or fatigue in achieving the longest cutting distance.

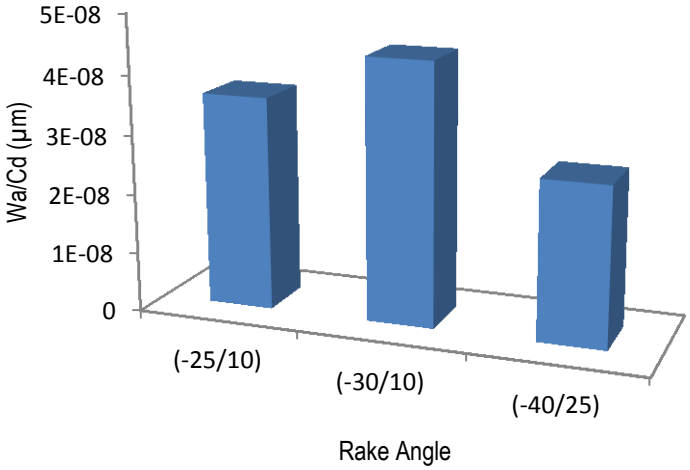

Fig. 17: Comparison of cutting tool wear resistance performance

While considering tool wear, a significant factor to consider is gradual tool degradation as a function of cutting distance. Fig. 17 shows comparison of the cutting tool wear resistance performance which is characterised as the ratio of tool wear area to cutting distance. Although the least ratio for (-40°) rake found in agreement with a previous study [37], which suggest less tool wear for large negative rake tools, the results don't constitute a direct proportionality relationship of decreasing tool wear with increasing negative rake angle. The tool with -30° rake found to undergo the highest tool wear than -40° as a function of cutting distance.

It was also noted that although observing the least frictional wear rate, diamond tool with -40° rake failed to maintain HPPT of silicon for longer cutting distance compared to -25° rake tool. This validates the importance of an optimal negative rake in machining brittle materials, where the worn tool can also machine in ductile regime using proper rake angle tool.

The effect of gradual tool wear can also be evaluated in the form of increased surface roughness of the machined surface. Fig. 18 presents the surface roughness

variation with respect to cutting distance. With the increasing cutting distance, the tool edge deteriorates and affects the machined surface. It can be noticed from the cutting force plot that major wear for all rake tools transpired before 20 km of cutting distance and then gradual frictional wear persisted for the remaining cutting distance. It is also interesting to note that at similar tool wear area, the DBT point changes as a function of rake angle. Due to the tool wear, insufficient hydrostatic stress level along with stress disproportionality under the cutting edge result in DBT of the material. Unlike -30° and -40° rake tools, -25° rake angle tool was found to generate required hydrostatic pressure for HPPT of silicon even in worn conditions.

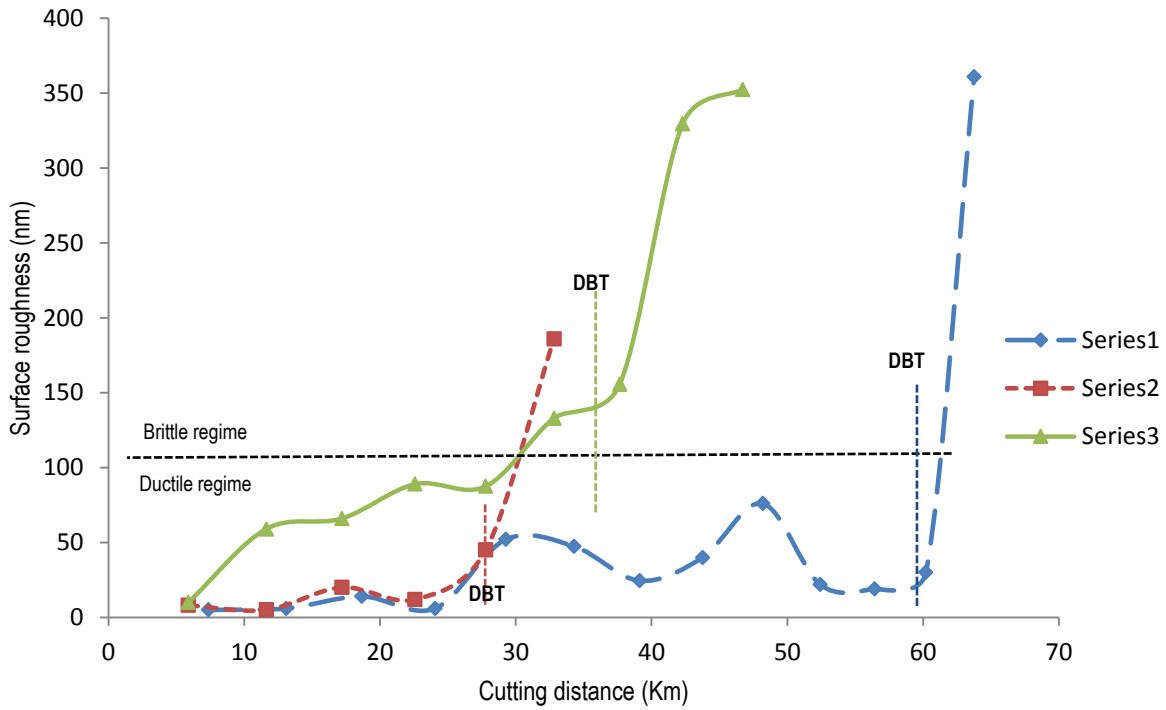

Fig. 18: Surface roughness trend with respect to cutting distance

7. Conclusion

The effect of tool rake angles was investigated in SPDT of silicon using experimental and simulation methods. The performance of diamond tools was analysed based on cutting forces, chip formation, surface roughness and tool wear studies. The analysis of these studies leads to the following conclusions:

- The mechanism of plastic deformation in SPDT of silicon reliant on pressure induced continuous material removal using negative rake angle tools. The material removal using positive rake tools procured in the form of cracks rather than continuous chip removal and final machined surface quality is dependent on crack direction.
- Surface roughness deteriorates with the increase of tool wear. However ductile mode machining can still be achieved with the worn tool provided the required hydrostatic pressure is maintained for HPPT of silicon during machining and this performance was found highly dependent on rake angles. Diamond tool with -25° rake angle maintained the longest ductile mode machining even undergoing higher frictional wear rate than -40° rake tool.
- The effect of rapid or progressive wear of diamond tool on HPPT of silicon varies for different rake angle tools. The tool with -30° rake angle was found to undergo the highest frictional resistance while cutting (111) silicon wafer and observed the shortest cutting distance than the other two tools. The relatively high tangential forces in experiments and reduction in shear plane length and lower von Mises stress in SPH simulation corroborate well for this behaviour.
- No direct correlation can be formed for tool performance with increasing or decreasing negative rake angle.

Acknowledgment

The authors gratefully acknowledge the financial support from the EPSRC (EP/K018345/1), Strathclyde University Impact Acceleration Account (120526/RA9029) and Royal Society-NSFC international exchange programme (IE141422) for this study.

References

1. Goel, S., et al., *Diamond machining of silicon: A review of advances in molecular dynamics simulation.* International Journal of Machine Tools and Manufacture, 2015. **88**: p. 131-164.
2. Kailer, A., Y.G. Gogotsi, and K.G. Nickel, *Phase transformations of silicon caused by contact loading.* Journal of Applied Physics, 1997. **81**(7): p. 3057.
3. Zhang, L. and I. Zarudi, *Towards a deeper understanding of plastic deformation in mono-crystalline silicon.* International Journal of Mechanical Sciences, 2001. **43**(9): p. 1985-1996.
4. Leung, T.P., W.B. Lee, and X.M. Lu, *Diamond turning of silicon substrates in ductile-regime.* Journal of Materials Processing Technology, 1998. **73**(1-3): p. 42-48.
5. Blake, P.N. and R.O. Scattergood, *Ductile-Regime Machining of Germanium and Silicon.* Journal of the American Ceramic Society, 1990. **73**(4): p. 949-957.
6. Chao, C.L.M., K. J.;Liu, D. S.;Bai, C. Y.;Shy, T. L., *Ductile behaviour in single-point diamond-turning of single-crystal silicon.* Journal of Materials Processing Technology, 2002. **127**(2): p. 187-190.
7. Yan, J.S., Katsuo;Kuriyagawa, Tsunemoto;Suzuki, Hirofumi, *Ductile regime turning at large tool feed.* Journal of Materials Processing Technology, 2002. **121**(2-3): p. 363-372.
8. Shibata, T., et al., *Ductile-regime turning mechanism of single-crystal silicon.* Precision Engineering, 1996. **18**(2-3): p. 129-137.
9. Fang, F.Z. and V.C. Venkatesh, *Diamond Cutting of Silicon with Nanometric Finish.* CIRP Annals - Manufacturing Technology, 1998. **47**(1): p. 45-49.
10. Uddin, M.S.S., K. H. W.;Rahman, M.;Li, X. P.;Liu, K., *Performance of single crystal diamond tools in ductile mode cutting of silicon.* Journal of Materials Processing Technology, 2007. **185**(1-3): p. 24-30.
11. Li, X.P.H., T.;Rahman, M., *Tool wear characteristics and their effects on nanoscale ductile mode cutting of silicon wafer.* Wear, 2005. **259**(7-12): p. 1207-1214.
12. Zong, W.J.S., T.;Li, D.;Cheng, K.;Liang, Y. C., *XPS analysis of the groove wearing marks on flank face of diamond tool in nanometric cutting of silicon wafer.* International Journal of Machine Tools and Manufacture, 2008. **48**(15): p. 1678-1687.
13. Patten, J.A. and W. Gao, *Extreme negative rake angle technique for single point diamond nano-cutting of silicon.* Precision Engineering, 2001. **25**(2): p. 165-167.
14. Limido, J., et al., *SPH method applied to high speed cutting modelling.* International Journal of Mechanical Sciences, 2007. **49**(7): p. 898-908.

15. Zhao, H., et al., *Influences of sequential cuts on micro-cutting process studied by smooth particle hydrodynamic (SPH).* Applied Surface Science, 2013. **284**: p. 366-371.
16. Gasiorek, D., *The Application of the Smoothed Particle Hydrodynamics (Sph) Method and the Experimental Verification of Cutting of Sheet Metal Bundles Using a Guillotine.* Journal of Theoretical and Applied Mechanics, 2013. **51**(4): p. 1053-1065.
17. R.A.Gingold, J.J.M., *Smoothed particle hydrodynamics theory and application to non spherical stars.* Royal Astronomical Society, 1977. **181**: p. 375-389.
18. Amrita Priyadarshinin, S.K.P., Arun K. Samantaray, *Finite Element modeling of chip formation in orthogonal machining*, in *Statistical and computational techniques in manufacturing*, J.P. Davim, Editor. 2012: London.
19. Aspinwall, D.K. and S.L. Soo, *Developments in modelling of metal cutting processes.* Proceedings of the Institution of Mechanical Engineers, Part L: Journal of Materials: Design and Applications, 2007. **221**(4): p. 197-211.
20. Ueda, K., et al., *A J-Integral Approach to Material Removal Mechanisms in Microcutting of Ceramics.* CIRP Annals - Manufacturing Technology, 1991. **40**(1): p. 61-64.
21. Xlet, J.Q.B.A.E.Z.H.M., *A study on shear banding in chip formation of orthogonal machining.* International Journal of Machine Tools and Manufacture, 1996. **36**(7): p. 835-847.
22. Obikawa, T., et al., *Application of Computational Machining Method to Discontinuous Chip Formation.* Journal of Manufacturing Science and Engineering, 1997. **119**(4B): p. 667-667.
23. Monaghan, J.J., *SPH without a Tensile Instability.* Journal of Computational Physics, 2000. **159**(2): p. 290-311.
24. M.Villumsen, T.F., *Simulation of metal cutting using smoothed particle hydrodynamics.pdf>.* LS-DYNA Anwenderforum, 2008. **Metallumformung III**(C-III): p. 17-36.
25. Daniel Charles Drucker, W.P., *Soil mechanics and plastic analysis or limit design.* Quarterly of Applied Mathematics, 1952. **10**(2): p. 157-165.
26. Simulia, *Abaqus User documentation.* softwar manual, 2014. **6.14**.
27. Durazo-Cardenas, I.S., P.;Luo, X.;Jacklin, T.;Impey, S. A.;Cox, A., *3D characterisation of tool wear whilst diamond turning silicon.* Wear, 2007. **262**(3-4): p. 340-349.
28. W.S.Blackley, R.O.S., *Ductile-regime machining model for diamond turning of brittle materials.* Precision Engineering, 1992. **14**(2): p. 118.
29. Ohta, T.Y., Jiwang;Yajima, Shuuma;Takahashi, Youichi;Horikawa, Naoyuki;Kuriyagawa, Tsunemoto, *High-efficiency machining of single-crystal germanium using large-radius diamond tools.* International Journal of Surface Science and Engineering, 2007. **1**(4): p. 374.
30. G.M.Ohrimenko, *Single crystal silicon piezoelectric ceramics and ferrite under uniaxial compression.* Tranlslated from Problemy Prochonosti, 1988. **9**: p. 45-50.
31. Mir, A., X. Luo, and A. Siddiq, *Smooth particle hydrodynamics study of surface defect machining for diamond turning of silicon.* The International Journal of Advanced Manufacturing Technology, 2016.
32. Cheung, C.F., S. To, and W.B. Lee, *Anisotropy of surface roughness in diamond turning of brittle single crystals.* Materials and Manufacturing Processes, 2002. **17**(2): p. 251-267.

33. Yan, J., H. Zhao, and T. Kuriyagawa, *Effects of tool edge radius on ductile machining of silicon: an investigation by FEM.* Semiconductor Science and Technology, 2009. **24**(7): p. 075018.
34. Goel, S., X. Luo, and R.L. Reuben, *Wear mechanism of diamond tools against single crystal silicon in single point diamond turning process.* Tribology International, 2013. **57**: p. 272-281.
35. Cai, M.B., X.P. Li, and M. Rahman, *Characteristics of "dynamic hard particles" in nanoscale ductile mode cutting of monocrystalline silicon with diamond tools in relation to tool groove wear.* Wear, 2007. **263**(7-12): p. 1459-1466.
36. Yan, J., K. Syoji, and J.i. Tamaki, *Some observations on the wear of diamond tools in ultra-precision cutting of single-crystal silicon.* Wear, 2003. **255**(7-12): p. 1380-1387.
37. Born, D.K. and W.A. Goodman, *An empirical survey on the influence of machining parameters on tool wear in diamond turning of large single-crystal silicon optics.* Precision Engineering, 2001. **25**(4): p. 247-257.